Proceedings of ASME Turbo Expo 2011
GT2011
June 6-10, 2011, Vancouver, British Columbia, Canada

GT2011-46596

TESTING OF A HYDROGEN DILUTE DIFFUSION ARRAY INJECTOR AT GAS TURBINE CONDITIONS

Nathan T. Weiland
National Energy Technology Lab
Pittsburgh, PA, USA
MAE Dept., West Virginia Univ.
Morgantown, WV, USA

Todd G. Sidwell
National Energy Technology Lab
Morgantown, WV, USA

Peter A. Strakey
National Energy Technology Lab
Morgantown, WV, USA

ABSTRACT

The U.S. Department of Energy's Turbines Program is developing advanced technology for high-hydrogen gas turbines to enable integration of carbon sequestration technology into coal-gasifying power plants. Program goals include aggressive reductions in gas turbine NOx emissions: less than 2 ppmv NOx at 15% oxygen and 1750 K firing temperature. The approach explored in this work involves nitrogen dilution of hydrogen diffusion flames, which avoids problems with premixing hydrogen at gas turbine pressures and temperatures. Thermal NOx emissions are partially reduced through peak flame temperature control provided by nitrogen dilution, while further reductions are attained by minimizing flame size and residence time.

The injector design includes high-velocity coaxial air injection from lobes surrounding the central fuel tube in each of the 48 array units. This configuration strikes a balance between stability and ignition performance, combustor pressure drop, and flame residence time. Array injector test conditions in the optically accessible Low Emissions Combustor Test & Research (LECTR) facility include air preheat temperatures of 500 K, combustor pressures of 4, 8 and 16 atm, equivalence ratios of 0.3 to 0.7, and three hydrogen/nitrogen fuel blend ratios.

Test results show that NOx emissions increase with pressure and decrease with increasing fuel and air jet velocities, as expected. The magnitude of these emissions changes deviate from expected NOx scaling relationships, however, due to active combustor cooling and array spacing effects. At 16 atm and 1750 K firing temperature, the lowest NOx emissions obtained is 4.4 ppmv at 15% O_2 equivalent (3.0 ppmv if diluent nitrogen is not considered), with a corresponding pressure drop of 7.7%. While these results demonstrate that nitrogen dilution in combination with high strain rates provides a reliable solution to low NOx hydrogen combustion at gas turbine conditions, the injector's performance can still be improved significantly through suggested design changes.

1 INTRODUCTION

The Integrated Gasification Combined Cycle (IGCC) power plant has become increasingly interesting to power producers due to its reduced footprint, and emissions controls, and its increased efficiency, relative to conventional coal-fired power plants. Reduction of CO_2 emissions can also be accommodated in such plants by water-gas shifting the syngas to a H_2/CO_2 mixture, separating and sequestering the CO_2, and burning the hydrogen fuel in the gas turbine. With an increase in the number of likely future IGCC installations with carbon capture and sequestration capabilities, pending regulation of CO_2 emissions, an opportunity exists to redesign the gas turbine combustor to more efficiently utilize high-hydrogen fuels.

Gas turbine combustion of syngas and high-hydrogen fuels is currently performed with swirl-based diffusion flames [1-6]. In fielded turbines, such combustors have been able to achieve NOx emissions as low as 12 ppm @ 15% O_2 [7], although nitrogen and steam dilution is used to reduce flame temperatures to achieve these emissions levels [8, 9]. While nitrogen is freely available from the air separation unit in an oxygen-blown IGCC plant (in roughly equal proportion to hydrogen fuel, by volume), the combustion products of high-hydrogen fuels already contain a lot of steam that causes heat transfer problems in the turbine, thus addition of steam diluent to the combustion chamber should be avoided [8].

Although these swirl-based diffusion flame combustors perform fairly well from an emissions perspective, additional NOx reductions are still sought after, and little optimization of these designs for high hydrogen combustion have been performed due to low market demand to date. Considerable research into premixed hydrogen combustion has been performed in recent years due to its promise of low NOx

emission; however, such combustion schemes are fairly intolerant of variations in the fuel content, and are also prone to the damaging effects of flashback and auto-ignition due to hydrogen's high flame speed.

As a middle ground, Lean Direct Injection (LDI) burners introduce fuel and excess air separately into the combustor, and rapidly mix them in an attempt to approach lean premixed flame conditions [10-17]. This combustion scheme avoids the flashback issues associated with true premixed combustion systems, while producing lower NOx emissions than traditional swirl-based combustors, though somewhat higher emissions than premixed combustors. The use of distributed injection schemes in LDI combustors represents an improvement, from a NOx emissions perspective, over traditional swirl-based combustors which utilize longer residence times to improve CO burnout, a feature not required for high-hydrogen combustion.

Among LDI burners, swirl-based designs were originally developed for liquid-fuelled aero-engines [11, 12], and have been recently modified to burn hydrogen fuel [13]. These hold some promise for reducing NOx emissions, though they remain prone to flame anchoring at elevated pressures [14]. Jet-based LDI injection schemes have also been studied [15, 16], most notably by Marek et al. at NASA [17], who investigated the potential of such schemes for low NOx combustion of hydrogen fuel at low equivalence ratios in aircraft gas turbine combustors. In the NASA study, the NOx emissions for several injectors from different manufacturers were tested, where the most promising schemes utilized arrays of small flames that also caused problems with overheating at the injector face.

Since most LDI designs are derived from aero-engine applications, few have studied the effect of dilution, with the notable exception of Ref. 16. It is likely, therefore, that reductions in NOx emissions can be realized by combining the dilution approach in land-based gas turbines with the low residence times of LDI-style injectors. This study shows that this combination can be effective at reducing NOx emissions in a jet-based hydrogen diffusion flame gas turbine combustor.

To provide some background on NOx emissions scaling in jet-based LDI combustors, previous scaling analyses of thermal NOx in a simple turbulent jet flame predict that $EINO_x$ scales as [18]:

$$EINO_x \propto t_{res} Da^{-n} \frac{d[NO]}{dt} \tag{1}$$

where t_{res} is the flame residence time and Da is the Damköhler number. The exponent on the Damköhler number scaling ranges from n = ½ at conditions where turbulence chemistry interactions prevail (low Da) to n = 0, where chemical reaction rates are much faster than mixing rates (high Da). The flame temperature primarily affects NOx production via the thermal NO production rate [19]:

$$\frac{d[NO]}{dt} \propto [O][N_2] e^{-38{,}370/T} \tag{2}$$

in which [O] and [N_2] are the molar concentrations of O-atoms and N_2 molecules, respectively, and T is the flame temperature, in Kelvins. The residence time for a jet flame, t_{res}, can be determined from the flame volume, V_f, divided by the volume flow rate of fuel leaving the jet exit, $U_F d_F^2$, where U_F and d_F are the jet exit velocity and diameter, respectively [18]. The flame volume is roughly proportional to the cube of the flame length, L_f, which is in turn proportional to d_F/f_s, where f_s is the stoichiometric mixture fraction [18], yielding a general NOx scaling of the form:

$$EINO_x \propto \frac{d_F}{U_F} \frac{Da^{-n}}{f_s^3} [O][N_2] e^{-38{,}370/T} \tag{3}$$

For simple jet flames, it has been shown that Da scales with the global flame strain, d_F/U_F, and that n = ½, so that $EINO_x \propto (d_F/U_F)^{1/2}$ [18-21]. In this case, NOx is reduced with small fuel jet diameters and high jet velocities, which leads naturally to an array-style injector design for low-NOx combustion. With the addition of high-velocity coaxial air flow, the flame volume and Damköhler number scalings change, but the same overall NOx scaling is retained, with higher velocities and smaller jet diameters resulting in lower NOx [18, 22].

The jet flame scaling of Eq. (3) also points to dilution of the fuel stream, rather than the air stream, as the most effective location for the nitrogen diluent in reducing NOx emissions. As a prior study has shown, the maximum peak flame temperature reduction is achieved with fuel dilution in lean diffusion flames, while flame volumes are also reduced through an order of magnitude increase in the stoichiometric mixture fraction, f_s [23]. This occurs because nitrogen displaces the amount of fuel to be burned, requiring less air entrainment per volumetric flow from the fuel jet, while the increased fuel jet momentum from dilution more efficiently entrains and mixes the air with the fuel. Further, due to diffusion of hydrogen out of the hydrogen/nitrogen fuel jet, flameholding and the flame's stability margins are improved such that higher velocities can be attained, leading to further reductions in NOx emissions [23].

Prior to designing an array-style injector, studies were performed on hydrogen/nitrogen jet flames with coaxial air at gas turbine conditions to determine the effects of pressure and air preheat temperature on flames of this type. In general, increasing pressure and/or air preheat temperature increases NOx emissions, flame stability, and combustion efficiency, as expected. These tests also reveal that NOx no longer scales with the Damköhler number at high pressures (n = 0) due to increased reaction rates, thus NOx emissions are directly proportional to the flame residence time [24].

A similar result was attained in atmospheric pressure streamtube tests, in which the dump plane of fuel and coaxial air jets were enclosed in an insulated tube to simulate a single injector in an array-style combustor. The lack of a Damköhler number scaling in this case may be due to consumption of generated NOx in the intense, entrainment-drive recirculation flows generated by this injector arrangement. In addition, the recirculation zones were found to cool the injector face at low equivalence ratios, while also improving combustion efficiency [25].

The streamtube combustor setup was also used to investigate alternative air injection strategies, as ignition and reattachment of the concentric tube coaxial air arrangement proved to be problematic at high velocity conditions. It was found that lobed air injection strategies offered improved stability characteristics without affecting the NOx emissions of the flame, thus it forms the basis for the design of the array style injector presented in this work.

The remainder of this paper discusses the design and construction of the array-style injector, the procedures utilized in testing this injector at representative gas turbine conditions, and the resulting NOx emissions, stability, and pressure loss performance at these conditions.

2 EXPERIMENTAL SETUP

2.1 Injector Design

The array injector is composed of 48 identical injector units, each with a central fuel jet with a diameter of d_F = 0.99 mm, and a lip thickness of 0.65 mm, surrounded by three coaxial air "lobes." The cross sectional area of the lobes, 166.4 mm^2, is chosen to yield a 2:1 fuel to air velocity ratio for a 50:50 H_2:N_2 fuel at an equivalence ratio of 0.7. In addition, the lobed geometry of the air injectors provide paths for the recirculation of combustion products back to the base of the fuel jet for ease of ignition, and are shaped to minimize the air-side pressure drop across the injector array. Specifically, at the design conditions of 8 atm combustion pressure, an inlet air velocity of 100 m/s at T_3 = 600 K , and 1:1 H_2:N_2 fuel jet velocity of 200 m/s at 450 K, the air-side pressure drop, $\Delta P/P$, for the as-specified air injector geometry was designed to be about 4%. As-built dimensions vary slightly from the design conditions, and should yield slightly lower pressure drops than the as-designed injector. Exit fuel and air Reynolds numbers at this design condition are about 43,000 and 10,000, respectively.

The array spacing was chosen as a balance between emissions performance and power, where wider spacing provides reduced NOx emissions and improved jet stability, while closer spacing yields higher thermal input per unit injector surface area. The arrangement of the array elements and the rotation of the air lobes was chosen to promote recirculation of combustion products, rather than air, into the base of the flame. The resulting distributor plate, fuel jet and air jet geometries are shown in Figure 1.

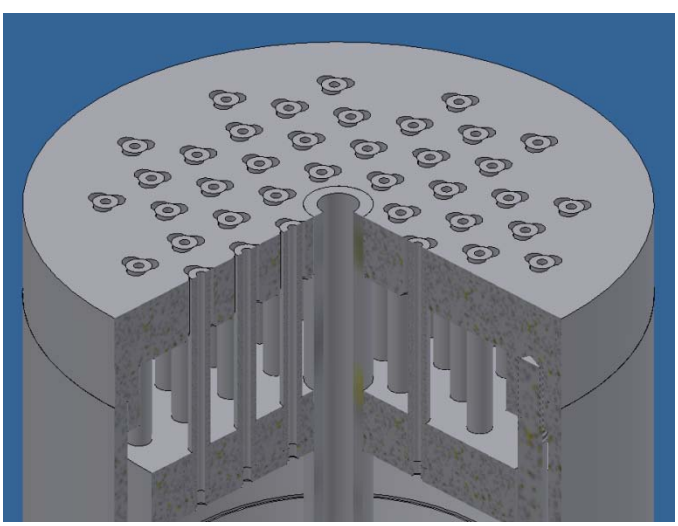

FIGURE 1: CUTAWAY RENDERING OF ARRAY INJECTOR (DISTRIBUTOR PLATE, AIR PLENUM AND FUEL TUBES)

2.2 Sim-Val Combustor Setup

The experiments were conducted in the NETL SimVal combustor, a 3 MWth research combustor which provides optical access to the combustion zone at pressures up to 20 atm. The combustor and pressure vessel geometries are shown in Figure 2. The pressure vessel allows optical access to the combustor through a maximum of four viewports, each of which provides a viewing area of 178 mm (width) x 305 mm (height). The combustor is scaled to be representative of a single gas turbine "can" combustor, with a clear, 180 mm ID, fused silica liner to allow optical access to the combustion zone. The lower portion of the fused silica liner is actively cooled by an array of impinging N_2 jets around the base of the liner. This cooling N_2 also provides a pressure balance across the liner, which is typically maintained at a differential pressure of 2 psid (external to the liner). The combustor features a long (60 cm) premixer section, which can be reconfigured to accommodate either premixed injectors or diffusion injectors of varying sizes. Additional information about this facility is available in Ref. 26.

These tests were conducted at pressures of 4, 8 and 16 atm, fuel jet velocities of 100, 150, 200, 250 and 300 m/s, nitrogen fuel dilution levels of 50, 33 and 23% by volume, and equivalence ratios ranging from 0.3 to 0.7. The combustor was supplied with preheated combustion air at flow rates of 24-290 g/s, H_2 at flow rates of 0.5-4.3 g/s at ambient temperature, and N_2 at flow rates of 7.0-60.5 g/s at ambient temperature.

This wide range of air flow rates is expected to cause variation in the air preheat temperature. When transitioning between significantly different flow conditions, heat transfer in

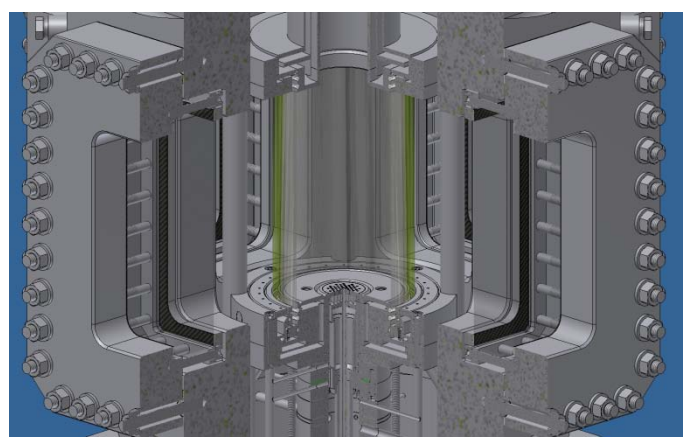

FIGURE 2: CUTAWAY RENDERING OF SIMVAL TEST SECTION AND COMBUSTOR WITH ARRAY INJECTOR

the air piping between the air preheater and the combustor becomes transient, thus causing variations in the air preheat temperature at the combustor. Varying the setpoint of the air preheater with each change in flow condition would result in impractically long test times, due to the time required to heat or cool the air piping to steady-state conditions. Thus, the preheat temperature is allowed to drift with each change in flow rate and is allowed to reach a different steady-state temperature.

The H_2-N_2 fuel mixture is supplied to the combustor through a central fuel supply plenum, while the combustion air is supplied through an annular air plenum, which fully surrounds the fuel plenum. This configuration results in significant heat transfer from the preheated combustion air to the fuel mixture, resulting in preheating the fuel mixture. Fuel and air temperature measurements are based on thermocouple measurements in the fuel and air plenums, with the last thermocouple set located 12.5 cm upstream of the injector tip and combustor dump plane. Details of the combustor and array injector configuration are shown in Figures 3 and 4. During the tests, air preheat temperatures of 455-555K and fuel preheat temperatures of 310-345K were measured at this location.

Additional heat transfer is expected to occur between the plenum thermocouples and the injector tip. The fuel and air jet temperatures at the injector tip are estimated iteratively during testing – based on measured flow rates, temperatures, and fuel compositions – and are used to continuously correct the target fuel and air jet velocities. Based on these corrections, air jet temperatures of 440-545K and fuel jet temperatures of 335-380K at the injector tip are estimated.

2.3 Instrumentation

Emissions are monitored during testing by continuously extracting a slipstream of process gas downstream of the combustor exhaust/burnout section for analysis by a mass spectrometer (for H_2, O_2, H_2O, N_2 and Ar species) and single-species analyzers for NO_X, and O_2. After the sample is extracted from the vessel, its pressure is reduced and the flow is split to allow the portion of the sample being supplied to the NO_X analyzer to pass through an NO_2-to-NO converter, which

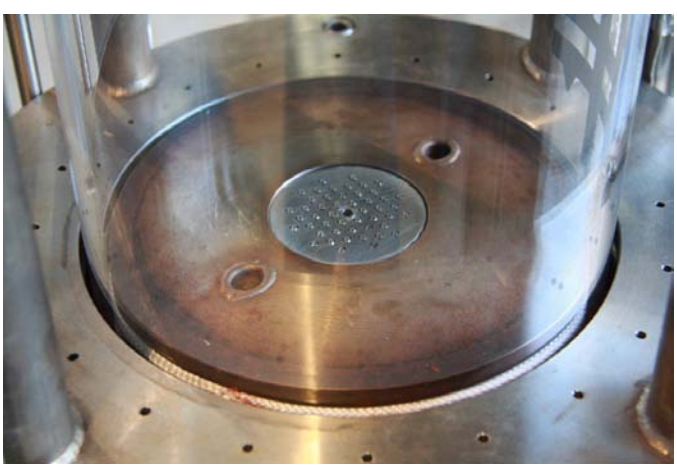

FIGURE 3: SIMVAL COMBUSTOR WITH ARRAY INJECTOR

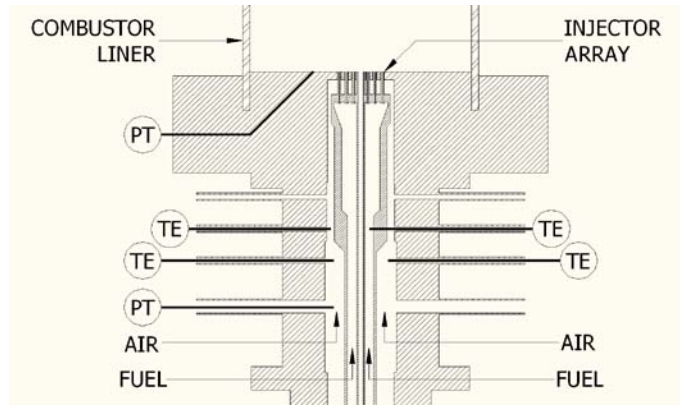

FIGURE 4: SCHEMATIC OF SIMVAL COMBUSTOR WITH ARRAY INJECTOR

converts water soluble NO_2 to less soluble NO. The sample streams then pass separately through a gas sample conditioner, which reduces the moisture content of the sample gas to less than 1% (vol) before being supplied to the analyzers. The NO_X analyzer has a selectable range and was set to measure 0-20 ppm (vol) during these tests, with a device accuracy of ±1% of reading. Previous experience has shown that the NO_X measurements are repeatable within ±0.5 ppm (vol).

A series of corrections and verifications are performed to ensure the quality of the measured data. Gas flow measurements are corrected with data obtained during annual calibration and flow proving. Historically, the corrections to the measured fuel flows amount to less than 1% of reading, and the corrections to the measured air and nitrogen flows amount to less than 2% of reading, due to the proven accuracy and repeatability of the flow measurement devices being used.

Measurements from the mass spectrometer and dedicated analyzers are used to calculate mass balances from a general chemical equation for complete combustion under lean conditions ($\varphi \leq 1$):

$$H_2 + \frac{1}{2\varphi}\left(O_2 + 3.7279N_2 + 0.0446Ar\right) + dN_2 \rightarrow H_2O + \left(\frac{1-\varphi}{2\varphi}\right)O_2 + \left(\frac{3.7279}{2\varphi} + d\right)N_2 + \frac{0.0446}{2\varphi}Ar \tag{4}$$

where ϕ is the equivalence ratio and d is the number of moles of nitrogen diluent per mole of hydrogen fuel.

The N_2/Ar ratio of the exhaust gas, β, is monitored by the mass spectrometer to provide an indication of any leakage of cooling N_2 into the combustor though the seals around the impingement cooled quartz liner. The total nitrogen diluent, d, from fuel dilution, d_{fuel}, and liner leakage, d_{leak}, can thus be determined from:

$$d = d_{fuel} + d_{leak} = \frac{0.0446\beta - 3.7279}{2\varphi_{flow}} \tag{5}$$

where φ_{flow} and d_{fuel} are determined from the air, nitrogen, and hydrogen flow controller outputs. Analysis of the results shows that d_{leak} ranges between 0.2 and 0.6, and therefore must be

considered when calculating NOx corrections. The total nitrogen dilution is used to correct raw NO_X measurements to 15% O_2 using [22, 23]:

$$\chi_{NOx,corr} = \chi_{NOx,meas}\left(\frac{0.2095-0.15}{0.2095-\chi_{O2,meas}}\right)\left(1+\frac{2(0.2095)}{1-0.2095}d\right) \quad (6)$$
$$= 6.6\times EINO_x$$

where χ_{NOx} and $\chi_{NOx,corr}$ are the NOx mole fraction (ppm) measurement and correction to 15% O_2, respectively, χ_{O2} is the measured dry product gas O_2 mole fraction, and *EINOx* is the emission index in units (g NO_2/kg H_2). The first part of Eq. (6) is the standard correction to 15% O_2 in the combustion products, while the last term in parentheses accounts for the diluent effect of nitrogen on the corrected NOx measurement, such that the same corrected NOx results if the diluent nitrogen is replaced by the same number of moles of air to yield 15% O_2 in the dry combustion products [23]. Note that this type of NOx correction follows the spirit of correcting to 15% O_2 in the exhaust gas, which was not originally meant to account for inert gas dilution. By strictly adhering to the 15% O_2 correction (setting d = 0 in Eq. 6), the "corrected NOx" can be artificially reduced by adding diluent to the combustor, though this practice is not followed in reporting the results of this study.

Finally, it should be noted that the equivalence ratio, φ, and the nitrogen dilution level, d, can also be calculated from the mass spec measurements of the nitrogen, oxygen, and argon in the product gases, and differ somewhat from those calculated with the flow controller outputs, as shown in Figure 5. These differences have been unresolved to date, and may be the result of inaccuracies in the flow controllers or mass spectrometer, or due to an unknown leak in the air inlet line. Results reported in the remainder of this work are based on the flow controller data, which are more conservative in that they correspond to lower firing temperatures for a given level of emissions, and a higher corrected NOx emission level, per Eq. (6).

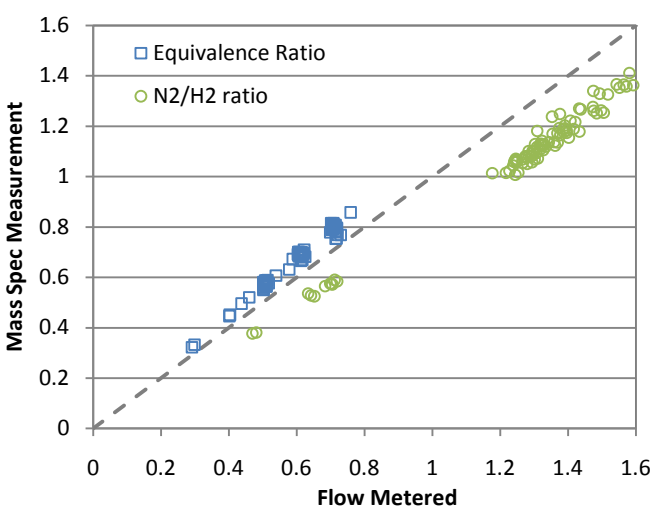

FIGURE 5: DIFFERENCES BETWEEN CALCULATED VALUES OF φ AND d, FROM FLOW CONTROLLER AND MASS SPECTROMETER OUTPUTS

3 RESULTS AND DISCUSSION

Images of the combustor in various states of operation, as captured from digital videos, are presented in Figure 6, where several notable features of the flame array are evident. First, rather than behaving as individual flames, in most cases the flames merge into a central flame zone about 1 cm downstream of the injector face. This is largely due to the close array spacing in the injector, but is also affected by the stability of individual flames. In particular, it can be seen that injectors on the outer edge of the array are not attached to the rim of the fuel tube due to entrainment of cooler combustion products from the large corner recirculation zone within the combustor, while flames nearer to the center of the array are more likely to be attached (e.g., Fig 6c). Distinction of individual flames and flame attachment is observed to increase with increasing pressure (not shown) and increasing equivalence ratio (Figs. 6e-6g), which is likely a result of increased reaction rates at higher pressures and temperatures. The overall length and width of the merged flame are not observed to change much, though luminosity increases at higher pressures, fuel flow rates (Figs. 6a-6c), and equivalence ratios (Figs. 6e-6g) as a result of increased temperatures due to reduced heat loss at these conditions. In some instances, a low-luminosity "tail" is seen to extend upwards from the central flame zone, and may either be an indicator of decreased mixing of combustion products with reactants at the lower velocity conditions (Fig. 6c), or may be due to a larger recirculation zone above the unused central

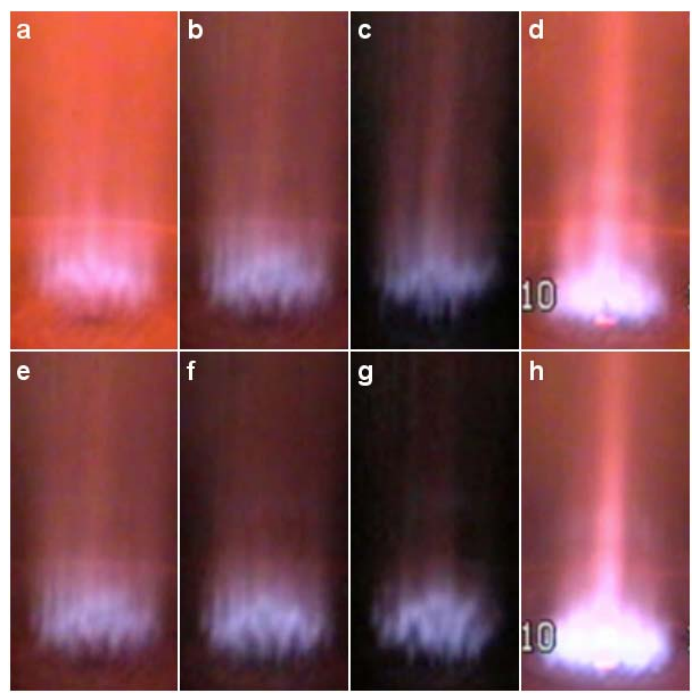

FIGURE 6: FLAME IMAGES AT 8 ATM FOR A) 50% N_2, U_F = 200 M/S, Φ = 0.7, B) 50% N_2, U_F = 150 M/S, Φ = 0.7, C) 50% N_2, U_F = 100 M/S, Φ = 0.7, D) 33% N_2, U_F = 150 M/S, Φ = 0.6, E) 50% N_2, U_F = 150 M/S, Φ = 0.7 (REPEAT), F) 50% N_2, U_F = 150 M/S, Φ = 0.6, G) 50% N_2, U_F = 150 M/S, Φ = 0.5, H) 23% N_2, U_F = 122 M/S, Φ = 0.5. THE WIDTH OF EACH IMAGE IS 5.7 CM.

pilot tube (Figs 6d & 6h).

With decreasing nitrogen content in the hydrogen fuel (Figs. 6f, 6d & 6h), the merged flame anchors much closer to the injector face and is reduced in length. Previous studies indicate that flame length typically increases with reduced nitrogen dilution due to a reduction in the momentum of the fuel jet and an increase in the amount of air required to complete combustion [19, 23]. However, the test conditions for the reduced diluent fuels targeted a constant fuel jet velocity and combustor exit temperature, thus resulting in higher air jet velocities relative to their more heavily diluted counterparts. A higher air to fuel velocity ratio is conducive to reduced flame lengths [18, 22-25], consistent with those observed in Fig. 6.

3.1 Stability and Combustion Efficiency

The following results are attained at static conditions, after all heat transfer and emissions transients had reached a steady state. In previous experiments, air flow was increased until a blowout or other flow limiting condition was reached [24], however, due to the preheating arrangement and the heat transfer between the air and fuel upstream of the injector, accurate calculation of the fuel and air jet velocities required that static data points be taken.

Previous experiments also used the mass spectrometer to measure the hydrogen concentration in the combustion products to determine the combustion efficiency, which typically decreased significantly prior to flame blowout [24]. Hydrogen concentrations in these experiments never exceeded background noise levels for the mass spectrometer, so combustion of the hydrogen can be considered complete in all experiments. This is likely due to the strong recirculation zones in the combustor, which also result in very stable combustor operation, as flame-induced blowouts were not observed during the course of the experiments.

3.2 Combustor Pressure Drop

The air-side pressure drop across the combustor is shown in Fig. 7, and is primarily a function of the air injection velocity, as expected. As mentioned above, the geometry of the air lobes was designed to yield about a 4% pressure drop at the design condition of 8 atm and 100 m/s air velocity, exactly the result shown in Fig. 7. This air velocity corresponds to $\varphi \approx 0.7$ and 0.55 at 200 and 150 m/s fuel jet velocity, respectively. Much of the scatter in the 4 atm pressure drop data can be attributed to variations in the air temperature at the exit of the injector.

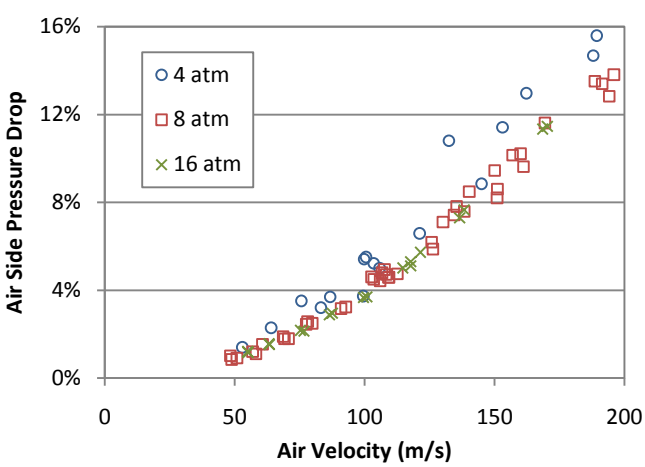

FIGURE 7: INJECTOR PRESSURE DROP

3.3 NOx Emissions Performance

Presented in Fig. 8 are the corrected NOx emissions versus equivalence ratio for all of the tests performed with 50% nitrogen dilution of the fuel. The scatter in the repeat NOx measurements is due to day-to-day variations in the operation of the combustor, and is indicative of the error in the emissions measurements. NOx is shown to generally increase with both pressure and equivalence ratio, as expected.

NOx reductions are expected with increasing fuel and air velocities as flame residence times are reduced per the scaling of Eq. 1, however, these reductions are not observed to a great extent in the 4 and 8 atm cases. The 16 atm cases do display these trends, however, particularly at low equivalence ratios. One reason for these differences is believed to be due to an increase in reaction rates at higher pressures, where a shift from the merged flame array behavior at low pressure to an array of individual flames yields the expected NOx scaling relationships for the individual flames.

The increase in reaction rates that precipitates this behavior

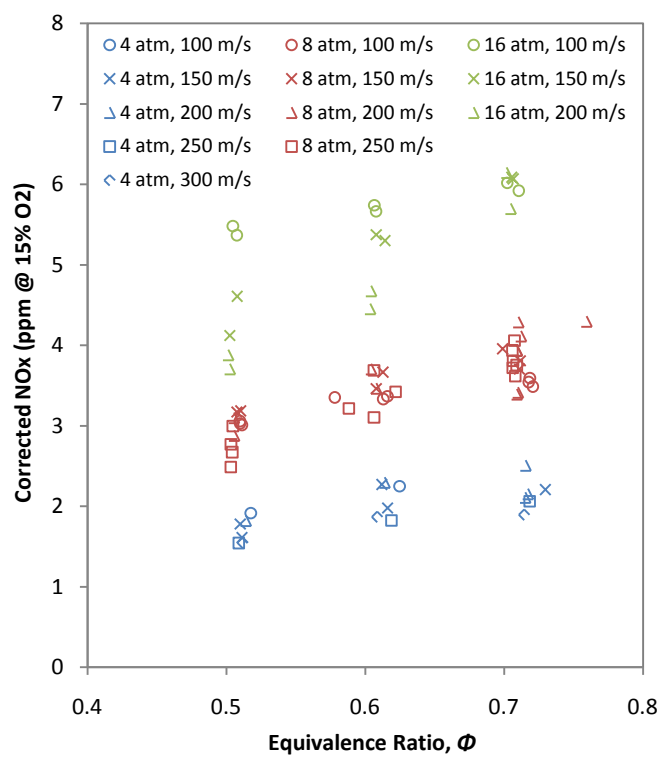

FIGURE 8: CORRECTED NOX EMISSIONS VS. EQUIVALENCE RATIO FOR 50% HYDROGEN DILUTION

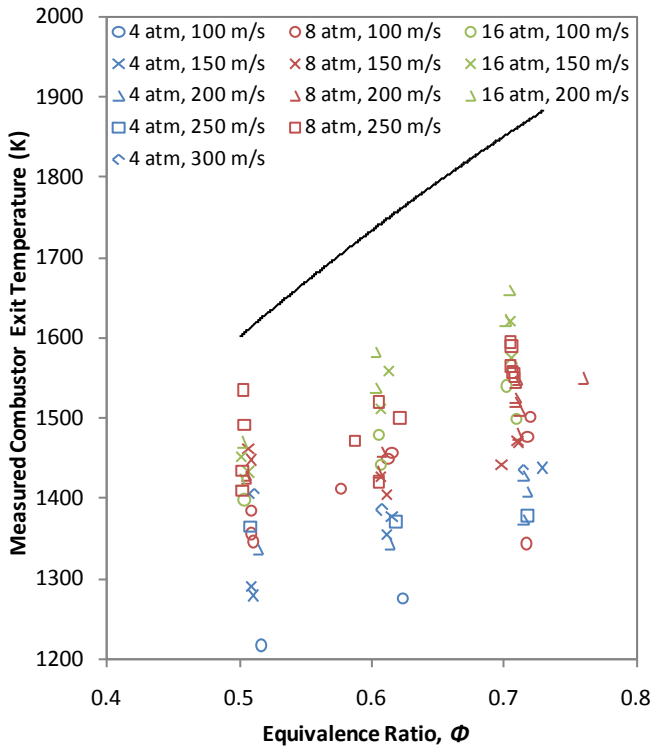

FIGURE 9: MEASURED COMBUSTOR EXIT TEMPERATURES VS. EQUIVALENCE RATIO FOR ALL 50% HYDROGEN DILUTION CASES

is due to both an increase in reaction rates with combustion chamber pressure, as well as a likely increase in the temperature of the combustion products recirculating to the base of the flame, since impingement cooling of the combustion liner becomes less effective at higher thermal loading in the combustor. This can be seen in Fig. 9, where measured combustor exit temperatures are shown to increase with pressure and fuel jet velocity, both of which increase the combustor's heat input. The effectiveness of the combustor cooling systems can be determined by comparing the measured exit temperature against a calculated adiabatic combustor exit temperature shown by the black line in Fig. 9.

These heat losses may also play a large role in determining the NOx emissions, as the temperature of the combustion products affect the flame temperature through recirculation, as well as any NOx production that occurs downstream of the flame zone. This may be a primary reason why NOx trends do not follow the expected residence time scaling at lower pressures, as increased temperatures at high velocities offset any residence time-related NOx reductions that might otherwise occur.

That the lower pressure cases do not display the expected NOx scaling with flame residence time is interesting, and may require further investigation. However, injector design changes that promote individual flame behavior, such as increasing the array spacing or fuel tube lip thickness, could be applied to result in similar NOx reductions at low pressure as at high pressure. In addition, in an actual combustor where heat losses

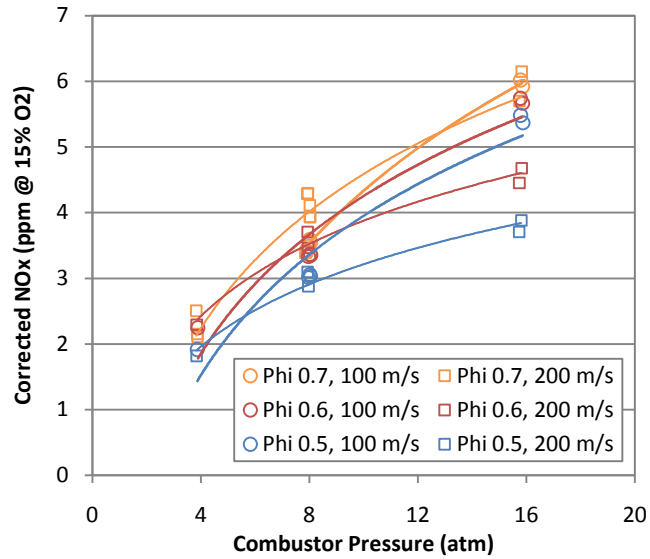

FIGURE 10: CORRECTED NOX EMISSIONS VS. COMBUSTION PRESSURE FOR 50% HYDROGEN DILUTION AND U_F = 100 & 200 M/S

are minimal and recirculation zones are much smaller, the emissions scaling would be expected to better follow the expected NOx scaling, where the above-mentioned heat loss effects are minimized.

The NOx emission trends with combustor pressure are also evident in Fig. 10, where larger decreases in NOx emissions with increasing fuel and air velocities are noted for higher pressures. The overall scaling of NOx with pressure is consistent with the results of previous studies of single coaxial air flames in the SimVal combustor and opposed flow diffusion flame calculations under high strain, which were found to be the result of increases in peak flame temperature with pressure at fixed strain rates [24]. The temperature effect on thermal NOx production more than offsets a reduction in O-atom concentrations due to three-body recombination reactions as pressure increases, while these same three-body reactions also initiate the N_2O formation route, further increasing NOx emissions at higher pressure [24].

Shown in Fig. 11 are the NOx emissions results of several tests performed with reduced levels of nitrogen diluent in the hydrogen fuel jet. The fuel jet velocity was fixed at 150 m/s in all cases, and attempts were made to match the combustor exit temperatures of the 50% nitrogen dilution cases by increasing the air velocity (lowering φ). The increasing NOx with reduction in the fuel nitrogen content are indicative of higher stoichiometric peak flame temperatures for diffusion flames, where adiabatic flame temperatures at $\varphi = 1$ and 8 atm for 50%, 33%, and 23% nitrogen dilutions are 2038, 2228, and 2313 K, respectively. Note again that NOx emissions better follow expected trends with respect to air velocities in the 16 atm cases, where individual flame behavior and reduced heat losses are more prevalent.

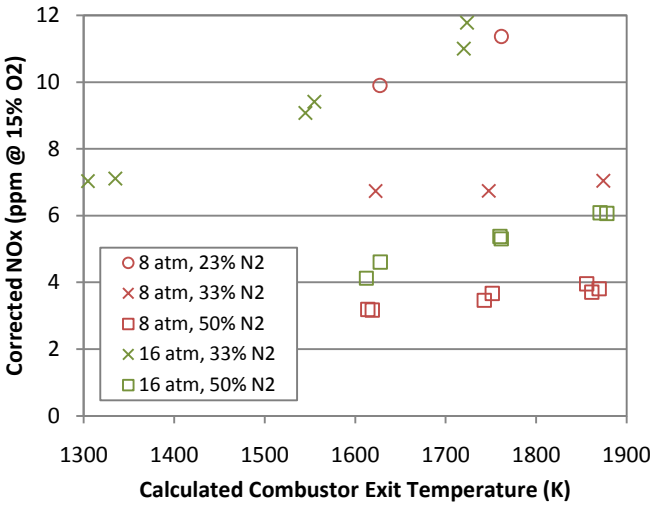

FIGURE 11: CORRECTED NOX EMISSIONS VS. COMBUSTION PRESSURE AND NITROGEN FUEL DILUTION LEVEL AT U_F = 150 M/S

4 CONCLUSIONS

Rigorous testing of the array injector in the SimVal combustor reveals that the injector yields very stable, complete combustion of the nitrogen diluted hydrogen fuel, in spite of high cooling rates and fuel and air velocities. Test results also show that NOx emissions increase with pressure and decrease with increasing nitrogen dilution, fuel velocity, and air velocity, as expected. The magnitude of the changes in NOx emissions are not entirely consistent with established NOx scaling relationships for simple jets with coaxial air flow. This is due in large part to a secondary effect of the active combustor cooling on the overall temperatures and NOx production in the combustor, and is not expected to play a role in a more realistic gas turbine combustor, where heat losses are minimal. In addition, there may be some effect of the array spacing on the NOx emissions results, where tightly spaced array injectors yield a merged flame that may not follow the same NOx scaling relationships as those of a single coaxial jet flame.

Finally, note that the goal of the program is to achieve stable combustion of high-hydrogen fuels at gas turbine conditions (16 atm, 1750 K firing temperature) with less than 2 ppm NOx @ 15% O_2. Under these conditions, the best emissions performance obtained with the array-style injector is 4.4 ppm NOx at a fuel jet velocity of 200 m/s and $\varphi \approx 0.6$, with a corresponding pressure drop of about 7.7%. It is also worth noting that correcting the emissions to the equivalent of 15% O_2 per Eq. 6 is following the spirit of the law rather than the letter of the law, where the nitrogen fuel diluent can be used to reduce the apparent NOx emissions while maintaining a 15% oxygen concentration in the exhaust gas. In such a correction, the total nitrogen diluent d in Eq. 6 is replaced by d_{leak} to simply account for coolant leakage into the exhaust gas, reducing the best emissions performance from 4.4 ppm NOx at the equivalent of 15% O_2, to 3.0 ppm NOx at exactly 15% O_2.

This work demonstrates that nitrogen dilution in combination with high strain rates is an effective method to reduce NOx emissions to levels below 6 ppm at realistic turbine firing temperatures. It should be noted that several improvements can still be made to this system to improve its NOx emissions performance. In particular, this study focuses on coaxial air injection to simplify the science involved, but more effective flame residence time reductions, and hence NOx and pressure drop reductions, can be achieved with angled air or fuel injection into the combustion zone. With the existing geometry, however, although the emissions are not quite as low as premixed systems (~ 3 ppm), this technology does present an attractive alternative to the intrinsic complexities and operability problems associated with premixed hydrogen combustion approaches.

ACKNOWLEDGMENTS

The authors gratefully acknowledge the support of Rich Dennis and the DOE Office of Fossil Energy's Advanced Hydrogen Turbine program. The authors also wish to thank Mark Tucker and Jeff Riley for assistance with and operation of the SimVal combustor, and Steve Beer for assistance with the mass spectrometer and gas sampling system.

REFERENCES

1. Vogt, R. L., 1980, "Low Btu coal gas combustion in high temperature turbines," ASME Paper No. 80-GT-170.
2. Beebe, K. W. and Blanton, J. C., 1985, "Design and development of a heavy-duty industrial gas turbine combustion system for low-Btu coal gas fuel," ASME Paper No. 85-GT-45.
3. Becker, B. and Schetter, B., 1993, "Use of LHV in a gas turbine," *Bioresource Technology*, **46**, 55-64.
4. Kelsall, G. J., Smith, M. A., and Cannon, M. F., 1994, "Low emission combustor development for an industrial gas turbine to utilize LCV fuel gas," *ASME J. Eng. Gas Turbines and Power*, **116**, 559-566.
5. Battista, R. A. and Dudley, J. C., 1995, "Full-scale F technology combustor testing of simulated coal gas," Final Report, DOE-MC/27221-1.
6. Reiss, F., Griffin, T., and Reyser, K., 2002, "The Alstom GT13E2 medium BTU gas turbine," ASME Paper No. GT-2002-30108.
7. Todd, D. M., and Battista, R. A., 2000, "Demonstrated applicability of hydrogen fuel for gas turbines," Proceedings of the IChemE "Gasification 4 the Future" Conference, Noordwijk, the Netherlands.
8. Chiesa, P., Lozza, G., and Mazzocchi, L., 2005, "Using hydrogen as gas turbine fuel," *ASME J. Eng. Gas Turbines and Power*, **127**, 73-80.
9. Todd, D. M., 2000, "Gas turbine improvements enhance IGCC viability," Gasification Technologies Conference, San Francisco, California.
10. Ziemann, J., Shum, F., Moore, M., Kluyskens, D., Thomaier, D., Zarzalis, N. and Eberius, H., 1998, "Low-

NOx combustors for hydrogen fueled aero engine," *Int. J. Hydrogen Energy*, **23**(4), 281-288.
11. Tacina, R. R., Wey, C., and Choi, K. J., 2001, "Flame tube NOx emissions using a lean-direct-wall-injection combustor concept," AIAA-2001-3271.
12. Tacina, R., Wey, C., Liang, P., and Mansour, A., 2002, "A low NOx lean-direct injection, multipoint integrated module combustor concept for advanced aircraft gas turbines," NASA/TM-2002-211347.
13. Hernandez, S. R., Wang, Q., McDonell, V., Mansour, A., Steinthorsson, E, and Hollon, B., 2008, "Micro-mixing fuel injectors for low emissions hydrogen combustion," ASME Paper No. GT2008-50854.
14. Hernandez, S., Wang, Q., Lee, H., McDonell, V., Hollon, B., Mansour, A., and Steinthorsson, E., 2008, "Micro-mixing fuel injection for low emission combustion of hydrogen for gas turbine applications," International Pittsburgh Coal Conference, Pittsburgh, PA, USA.
15. Dahl, G., and Suttrop, F., 1998, "Engine control and low-NOx combustion for hydrogen fuelled aircraft gas turbines," *Int. J. Hydrogen Energy*, **23**(8), 695-704.
16. GE Energy, 2005, "Premixer design for high hydrogen fuels – Final report," DOE Cooperative Agreement No. DE-FC26-03NT41893.
17. Marek, C. J., Smith, T. D., and Kundu, K., 2005, "Low emission hydrogen combustors for gas turbines using lean direct injection," AIAA-2005-3776.
18. Chen, R.-H. and Driscoll, J. F., 1990, "Nitric oxide levels of jet diffusion flames: effects of coaxial air and other mixing parameters," *Proc. Combust. Instit.*, **23**, 281-288.
19. Turns, S. R., 1995, "Understanding NO_x formation in nonpremixed flames: experiments and modeling," *Prog. Energy Combust. Sci.*, **21**, 361-385.
20. Gabriel, R., Navedo, J. E., and Chen, R.-H., 2000, "Effects of fuel Lewis number on nitric oxide emissions of diluted H_2 turbulent jet diffusion flames," *Combust. Flame*, **121**, 525-534.
21. Chen, J.-Y., and Kollmann, W., 1992, "PDF modeling and analysis of thermal NO formation in turbulent nonpremixed hydrogen-air jet flames," *Combust. Flame*, **88**, 397-412.
22. Weiland, N., Chen, R.-H., and Strakey, P., 2010, "Effects of coaxial air on nitrogen-diluted hydrogen jet diffusion flame length and NOx emission," *Proc. Combust. Inst.*, doi:10.1016/j.proci.2010.06.075.
23. Weiland, N. T., and Strakey, P. A., 2010, "NOx reduction by air-side versus fuel-side dilution in hydrogen diffusion flame combustors, *J. Eng. Gas Turbines and Power*, **132**(7): 071504.
24. Weiland, N. T., Sidwell, T. G., and Strakey, P. A., "Effect of pressure and air preheating on dilute hydrogen jet diffusion flames with coaxial air injection," 2010 Spring Technical Meeting, Central States Section/Combustion Institute, Champaign IL, March 21-23, 2010.
25. Weiland, N. T., and Strakey, P. A., "Flame structure and NOx scaling of confined dilute hydrogen diffusion flames," 2010 Spring Technical Meeting, Central States Section/ Combustion Institute, Champaign IL, March 21-23, 2010.
26. Sidwell, T., Richards, G., Casleton, K., Straub, D., Maloney, D., Strakey, P., Ferguson, D., Beer, S., and Woodruff, S., "Optically Accessible Pressurized Research Combustor for Computational Fluid Dynamics Model Validation" *AIAA Journal*, Vol. 44, No. 3, March, 2006, pp. 434-443.